



# HOKKAIDO UNIVERSITY

Title	Influence of vacuum annealing conditions on the surface oxidation and vacancy condensation in the surface of an FeAl single crystal
Author(s)	Yamauchi, A.; Tsunekane, M.; Kurokawa, Kazuya et al.
Citation	Intermetallics, 18(4), 412-416 <a href="https://doi.org/10.1016/j.intermet.2009.08.014">https://doi.org/10.1016/j.intermet.2009.08.014</a>
Issue Date	2010-04
Doc URL	<a href="https://hdl.handle.net/2115/42971">https://hdl.handle.net/2115/42971</a>
Type	journal article
File Information	Int18-4_412-416.pdf



Influence of vacuum annealing conditions on the surface oxidation and vacancy condensation in the  
surface of an FeAl single crystal

A. Yamauchi<sup>1\*</sup>, M. Tsunekane<sup>2</sup>, Kazuya Kurokawa<sup>1</sup>

Shuji Hanada<sup>3</sup> and Kyosuke Yoshimi<sup>4</sup>

<sup>1</sup> Center for Advanced Research of Energy Conversion Materials, Hokkaido University, Sapporo

060-8628, Japan

<sup>2</sup> Graduate school student, Graduate School of Environmental Studies, Tohoku University, Sendai

980-8579, Japan (Present address: Materials Science and Engineering, University of Michigan)

<sup>3</sup> Institute for Materials Research, Tohoku University, Sendai 980-8577, Japan

<sup>4</sup> Graduate School of Environmental Studies, Tohoku University, Sendai 980-8579, Japan

\* Corresponding author; Akira Yamauchi, Tel:81-11-706-6818, Fax:81-11-706-7119, E-mail:  
akira-y@eng.hokudai.ac.jp, Address; Center for Advanced Research of Energy Conversion  
Materials, Hokkaido University, Kita 13 Nishi 8, Kita-ku, Sapporo 060-8628, Japan

## 1. Introduction

B2-type intermetallic compounds such as FeAl, NiAl, CoAl, and TiCo contain a high concentration of supersaturated thermal vacancies up to several mole percent [1 – 3]. One of reasons for the importance of residual thermal vacancies in B2-type FeAl is their large influence on its mechanical properties [4 – 7]. Recently, we reported the mesopore formation near the surface of B2-type FeAl [8 – 11]. Based on the results, we concluded that this pore formation was caused by the condensation of supersaturated thermal vacancies. On the other hand, the fact that the vacancy condensation near surface is affected by surface oxidation has been discussed so far [12 – 16]. In particular,  $\text{Al}_2\text{O}_3$  former intermetallic compounds such as NiAl,  $\text{Ni}_3\text{Al}$  [17 – 20] and FeAl [21, 22] form large cavities at scale/substrate interfaces. Al atoms in such aluminides are consumed for the formation of an  $\text{Al}_2\text{O}_3$  scale during high temperature oxidation. Thus, the oxidation-induced outward-cation diffusion and/or unequal diffusion of alloying elements in the substrates has been suggested as the mechanism responsible for the cavity formation. However, in our previous work [23], it was found that the thickness of an oxide layer formed on FeAl during vacuum annealing is almost the same as that of the passive film formed on an Al foil irrespective of the mesopore formation. Therefore, the surface oxidation seems not to be the main cause of the mesopore formation, but its influence on the mesopore formation and growth is still unclear at present. It is therefore important to understand the influence of the surface oxidation of FeAl during vacuum annealing on the formation and growth of mesopores.

Therefore, the objective of the present work is to investigate the effect of annealing conditions on the surface oxidation and vacancy condensation in the surface of FeAl single crystals. The annealing was performed under two levels of vacuum; about  $10^{-3}$  Pa (a high vacuum) and about  $10^{-6}$  Pa (an ultra high vacuum). The influence of surface oxidation on the mesopore formation and growth will be discussed on the basis of the results obtained.

## 2. Experimental Procedures

Fe-48mol%Al button ingots were prepared from 99.99mass% electrolytic iron and 99.99mass% aluminum by an arc-melting technique in an argon gas atmosphere. An FeAl single crystal was grown from these ingots by the Bridgman method. The chemical analysis of this single crystal indicated that its composition was approximately Fe-48.5mol%Al. After homogenization at 1373 K for 172.8 ks under a high vacuum, the single crystal was slowly cooled down to room temperature at a rate of  $5 \times 10^{-3} \text{ K}\cdot\text{s}^{-1}$  to avoid the introduction of a high concentration of supersaturated vacancies. {111}-oriented single crystal plates with a thickness of 1 mm were cut from the single crystal by electro-spark machining. They were kept at 1273 K for 3.6 ks in air, and then quenched into iced water to introduce supersaturated thermal vacancies. The surfaces of the quenched plate specimens were ground to remove the oxide scale formed during the heat treatment. The ground surfaces were further polished with diamond slurry and subsequently electropolished in a solution of  $\text{CH}_3\text{OH} : \text{HNO}_3 = 2 : 1$  to remove residual strain near the surfaces [24]. Moreover, the surfaces were plasma-cleaned first in an oxygen atmosphere and next in an argon atmosphere using South Bay Technology PE-2000. Finally, the plate specimens were annealed for up to 360 ks between 623 and 1023 K under a high vacuum of about  $5 \times 10^{-4} \text{ Pa}$  on the top of Ti powder as an oxygen getter, or under an ultra-high vacuum of about  $3 \times 10^{-6} \text{ Pa}$ . A thin  $\text{Al}_2\text{O}_3$  film formed on the FeAl surface and covered it during the annealing. This oxide film was removed by  $\text{Ar}^+$  ion milling under the condition as follows: primary ion beam energy was 3.5 kV, beam current 3 mA, beam angle with respect to the normal on the average surface plane  $15^\circ$ . Auger electron spectroscopy (AES, JEOL JAMP-7100E) with  $\text{Ar}^+$  ion sputtering was carried out to examine the surface composition and to obtain depth profiles of the relevant elements for the annealed specimens. The AES conditions were described in our previous paper [23]. The surface morphology of specimens was obtained by scanning electron microscopy (SEM) and atomic force microscopy (AFM). The oxide films formed on the annealed specimens were also observed by a transmission electron

microscopy (TEM) at an acceleration voltage of 200 kV. The diffraction patterns obtained were analyzed with Crystal Kit.

### 3. Results and Discussion

Fig. 1 shows an AFM micrograph of a specimen annealed at 873 K for 360 ks under a vacuum of  $5 \times 10^{-4}$  Pa. In this micrograph, rugged surface morphology is observed. Since the specimen surface before the annealing was flatter and smoother than that shown in this figure, it is obvious that the rugged surface was formed during the annealing. Fig. 2 shows the AES depth profiles of a specimen annealed at 873 K for 360 ks under a vacuum of  $5 \times 10^{-4}$  Pa. The Ar ion sputtering rate is about  $1 \times 10^{-8}$  m s<sup>-1</sup> in the case of SiO<sub>2</sub> layer grown on Si. From the sputtering time of zero, i.e., just surface, the concentration of oxygen decreases with increasing sputtering time for up to 200s beyond which it remains almost constant and very low level. This means that an oxide layer was formed on the top of the FeAl surface during the annealing. The concentration of aluminum is much higher than that of iron within the oxide layer. The relative concentration of iron increases with increasing sputtering time, and becomes higher than that of aluminum beyond 200 s, where it's almost constant at the higher level. Consequently, the difference between aluminum and iron in AES profiles strongly suggests that an Al<sub>2</sub>O<sub>3</sub> or an aluminum-rich oxide film was formed on the FeAl single crystal during the annealing. In this paper, the oxide-metal interface was defined as the point at which the oxygen concentration reaches the oxygen level in the FeAl single crystal substrate.

The oxide film mentioned above was also observed by TEM. Thin foils for TEM observations were prepared by one-side electropolishing with the other side kept intact. Fig. 3(a) shows a bright-field TEM image of a specimen annealed at 723 K for 3.6 ks under a vacuum of  $5 \times 10^{-4}$  Pa. The lower right area corresponds to a hole opened up by the electropolishing and the upper left area to the FeAl substrate. The un-electropolished surface, as expected above, was covered with

a thin oxide film over all even on the hole, while a small amount of triangular pores are seen in the upper left FeAl substrate. The pore patterns are based on a crystallographic configuration in which the pore surfaces are faceted to the {001} planes. For the {111}-oriented FeAl surface, the pore patterns are made up of regular triangles, so that the pore shape can be well defined as a triangular pyramid. The thin film formed was identified as metastable  $\kappa$ -Al<sub>2</sub>O<sub>3</sub> from the analysis of the electron diffraction pattern inserted in Fig. 3(a). Fig. 3(b) is a schematic diagram of the diffraction patterns illustrated by Crystal Kit, indicating that a thin {001}  $\kappa$ -Al<sub>2</sub>O<sub>3</sub> film epitaxially grew on the {111} FeAl surface. It is unclear whether this epitaxial relationship and the Al<sub>2</sub>O<sub>3</sub> structure remain when the oxide further grows.

From the TEM observations, it was found that the  $\kappa$ -Al<sub>2</sub>O<sub>3</sub> film covered the surface of the FeAl surface and hence prevented the observation of surface mesopores by AFM. In order to remove the  $\kappa$ -Al<sub>2</sub>O<sub>3</sub> film, Ar<sup>+</sup> ion milling as conventionally done for TEM sample preparation was conducted at 3.5 kV and at an incidence angle of 15 deg. Fig. 4 shows an AFM micrograph of the surface of a specimen annealed at 873 K for 360 ks under a vacuum of  $5 \times 10^{-4}$  Pa followed by Ar<sup>+</sup> ion milling for 30 s. Various-sized triangular pores are homogeneously distributed in the surface in this figure. This surface morphology is in good agreement with that observed in our previous works [8 – 11]. Therefore, it was confirmed that the  $\kappa$ -Al<sub>2</sub>O<sub>3</sub> film formed during the annealing can be removed easily with a mild milling for a short time. A passive Al<sub>2</sub>O<sub>3</sub> film should be formed again after the Ar<sup>+</sup> ion milling in the ambient atmosphere (as shown in Fig. 5). The passive film on FeAl and Al are referred from our previous result [23]. The passive Al<sub>2</sub>O<sub>3</sub> film formed again on the FeAl surface should be thinner than that formed on Al.

In the case of high temperature oxidation, it is well known that Al atoms in aluminides are consumed for the formation of a protective Al<sub>2</sub>O<sub>3</sub> scale on their surface and metal atoms other than aluminum near the surface simultaneously diffuse toward the aluminide matrix due to a large chemical potential gradient. Consequently, the Al concentration in the aluminide matrix decreases

by the oxidation. Furthermore, voids are commonly observed at the oxide/alloy interfaces as a result of the so-called Kirkendall effect [17 – 22]. These phenomena are also likely to occur in this study. The condensation of supersaturated vacancies and voids formation by surface oxidation could cause the surface mesopore formation. However, the surface mesopore formation dealt with in this study never occurred in our previous study [11] where supersaturated vacancies were fully removed from FeAl. This is the grounds why we conclude that the surface mesopore formation is caused by the annihilation of supersaturated vacancies.

Based on the above discussion, we considered that the surface oxidation may have influence on the growth of surface mesopores. Thus, the relationship between the annealing temperature, time and the oxide film thickness was investigated in the temperature range of 623 – 1023 K for up to 86.4 ks. Fig. 6 shows the annealing temperature dependence of the thickness in terms of sputtering time of the Al<sub>2</sub>O<sub>3</sub> film formed by the annealing in a vacuum of about  $5 \times 10^{-4}$  Pa for 3.6 to 86.4 ks. The thickness of a passive Al<sub>2</sub>O<sub>3</sub> film formed on FeAl at room temperature is also shown in this figure for comparison. The thickness of the Al<sub>2</sub>O<sub>3</sub> film gradually increases with increasing temperature. It is noteworthy that the thickness is independent of time below about 900 K. Above 900 K the thickness is also dependent on annealing time. This change in thickness between below and above 900 K can be caused by the promotion of Al diffusion during the vacuum annealing. Thus, the vacuum annealing above 900 K would influence the growth of oxide layer. On the other hand, the thickness of oxide layers formed at and below 900 K were unaffected by the vacuum annealing time. The influence of the degree of vacuum was similarly examined. The results are shown in Fig. 7. Under a vacuum of about  $5 \times 10^{-4}$  Pa, the growth of the oxide film obeys the logarithmic-rate law featuring for an ultra-thin oxide film. The thickness under about  $5 \times 10^{-4}$  Pa increases with the temperature rises, but that under about  $3 \times 10^{-6}$  Pa varies very slightly with temperature and annealing time and is almost the same as that of the passive film formed on the FeAl specimen. Therefore, we can conclude that the oxide film formed under the ultra-high vacuum

hardly grows during the annealing. FeAl substrate under the ultra-high vacuum formed a thin  $\text{Al}_2\text{O}_3$  film equivalent to a passive  $\text{Al}_2\text{O}_3$  film. The higher vacuum atmosphere has a negligible effect on the surface oxidation of FeAl during vacuum annealing. It is suggested that FeAl substrate annealed under the lower vacuum is affected by the diffusion flux of vacancy caused by oxidation.

The influence of the degree of vacuum on the formation characteristics of mesopore was examined by TEM. Fig. 8 shows bright-field TEM images of the specimens annealed under different vacua. From the images in this figure, it is indicated that the annealing under the high vacuum leads to the condensation of more vacancies than that under the ultra-high vacuum. This means that the surface oxidation of FeAl under the high vacuum annealing would assist the condensation of supersaturated vacancies and the growth of mesopores. These results demonstrate that the growth of surface mesopores is attributable to both the condensation of supersaturated vacancies in FeAl substrate and the Kirkendall effect by the surface oxidation during the vacuum annealing.

#### 4. Conclusions

In this study, the surface oxidation of FeAl single crystals during vacuum annealing under various conditions was investigated by AES, TEM, and AFM. The specimens contained thermally supersaturated vacancies before the vacuum annealing. The following conclusions were obtained.

- (1) The oxide film formed on {111}-oriented FeAl single crystals is {001}-oriented  $\kappa\text{-Al}_2\text{O}_3$ .
- (2) The thick  $\text{Al}_2\text{O}_3$  layer formed for a long time under a high vacuum affects the morphology of surface mesopores because the oxide layer covers the surface of the FeAl substrates.
- (3) The thickness of the oxide film increases slightly with the annealing time under a high vacuum of about  $5 \times 10^{-4}$  Pa. However, it hardly varies with the temperature and time under an ultra-high vacuum of about  $3 \times 10^{-6}$  Pa.

(4) The condensation of vacancies to form surface mesopores is more significant for the annealing under the high vacuum than under the ultra-high vacuum.

## Abstract

The influence of annealing atmosphere, temperature and time on the surface oxidation and vacancy condensation behavior of {111}-oriented single crystals of B2-type FeAl was investigated. AFM observation showed that as-annealed surfaces under a high vacuum were rugged and covered with a thin oxide film. The results obtained by TEM indicated that the thin oxide film was {001}-oriented  $\kappa$ -Al<sub>2</sub>O<sub>3</sub> epitaxially grown on the {111}-oriented FeAl surface. AES measurements showed that the thickness of the oxide film was almost twice as thick as that of the passive Al<sub>2</sub>O<sub>3</sub> film formed on the FeAl surface in an ambient atmosphere. It was found that the growth of surface mesopores is attributable to both the condensation of supersaturated vacancies in FeAl substrate and the Kirkendall effect by the surface oxidation during the vacuum annealing.

Keywords; A. Iron aluminides, B. oxidation, D. defect: point defect, F. microscopy, various

## **Acknowledgements**

The authors would like to thank Mr. Y. Murakami for the technical support in the AES measurements at the Laboratory for Advanced Materials, Tohoku University. The authors express their sincere thanks to Prof. S. Taniguchi for criticizing the draft of this paper. This work was performed under the inter-university cooperative research program of the Institute for Materials Research, Tohoku University, and supported by a Grant-in-Aid for Science Research from the Ministry of Education, Culture, Sports, Science and Technology of Japan under Contract No. 16360339.

## Figure captions

Fig. 1 AFM micrograph of the surface of a {111}-oriented FeAl single crystal after annealing at 873 K for 360 ks under a vacuum of  $5 \times 10^{-4}$  Pa.

Fig. 2 Auger depth profiles of the relevant elements for the FeAl single crystal annealed at 873 K for 360 ks under a vacuum of  $5 \times 10^{-4}$  Pa. Solid diamond: oxygen, open square: aluminum, solid circle: iron.

Fig. 3 (a) Bright-field TEM image and (b) schematic diffraction pattern of the FeAl single crystal, annealed at 723 K for 3.6 ks under a vacuum of  $5 \times 10^{-4}$  Pa.

Fig. 4 AFM micrograph of the surface of the FeAl specimen sputtered with Ar ion beam to remove the surface oxide, after annealing at 873 K for 360 ks under a vacuum of  $5 \times 10^{-4}$  Pa.

Fig. 5 Auger depth profiles of the relevant elements for the FeAl single crystal annealed at 873 K for 360 ks under a vacuum of  $5 \times 10^{-4}$  Pa, and then subjected to Ar ion milling. Solid diamond: oxygen, open square: aluminum, solid circle: iron.

Fig. 6 Variation of the oxide film thickness (in terms of sputtering time) with annealing temperature as a function of annealing time. Under a vacuum of about  $5 \times 10^{-4}$  Pa. Circle: 3.6 ks, square: 18 ks, diamond: 36 ks, triangle: 86.4 ks.

Fig. 7 Variation of the oxide film thickness (in terms of sputtering time) with annealing time as a function of annealing temperature. Open symbols are obtained under a vacuum of about  $5 \times 10^{-4}$  Pa

and solid symbols a vacuum of about  $3 \times 10^{-6}$  Pa: Circle: 723 K, square: 873 K, and triangle: 1023K.

Fig. 8 Bright-field TEM images of the FeAl single crystals after annealing at 723 K for 36 ks under a vacuum of (a) about  $5 \times 10^{-4}$  Pa and (b) about  $3 \times 10^{-6}$  Pa.

## REFERENCES

- [1] Kerl R, Wolff J, Hehenkamp T. *Intermetallics* 1999;7:301.
- [2] Kogachi M, Haraguchi T. *Mater Sci Eng A* 1997;230:124.
- [3] Sung MS, Haraguchi T, Yoshimi K, Hanada S. *Mater Sci Forum* 2003;426-432:3727.
- [4] George EP, Baker I. *Intermetallics* 1998;6:759.
- [5] Yoshimi K, Hanada S, Yoo MH. *Acta Metall Mater.* 1995;43:4141.
- [6] Yoshimi K, Hanada S, Yoo MH. *Intermetallics* 1996;4:159.
- [7] Jordan JL, Deevi SC. *Intermetallics* 2003;11:507.
- [8] Yoshimi K, Hanada S, Haraguchi T, Kato H, Inoue A. *Mater Trans* 2002;43:2897.
- [9] Haraguchi T, Yoshimi K, Yoo MH, Kato H, Hanada S, Inoue A. *Acta Mater* 2005;53:3751.
- [10] Yoshimi K, Kobayashi T, Yamauchi A, Haraguchi T, Hanada S. *Philos Mag* 2005;85:331.
- [11] Yoshimi K, Tsunekane M, Nakamura R, Yamauchi A, Hanada S. *Appl Phys Lett* 2006;89:073110-1.
- [12] Kasen MB, Taggart R, Polonis DH. *Philos Mag* 1966;13:453.
- [13] Herbjornsen OH, Astrup T. *Philos Mag* 1969;19:693.
- [14] Parthasarathi A, Fraser HL. *Philos Mag* 1984;50:101.
- [15] Vanbeek HJ, Mittemeijer EJ. *Thin Solid Films* 1984;122:131.
- [16] Jawarani D, Kawasaki H, Yeo IS, Rabenberg L, Stark JP, Ho PS. *J Appl Phys* 1997;82:1563.
- [17] Kuenzly JD, Douglass DL. *Oxid Met* 1974;8:139.
- [18] Brumm MW, Grabke HJ. *Corros Sci* 1993;34:547.
- [19] Bobeth M, Bischoff E, Schumann E, Rockstroh M, Ruhle M. *Corros Sci* 1995;37:657.
- [20] Hou PY, Priimak K. *Oxid Met* 2005;63:113.
- [21] Grabke HJ. *Intermetallics* 1999;7:1153.
- [22] Hou PY, Niu Y, Lienden CV. *Oxid Met* 2003;59:41.
- [23] Yamauchi A, Yoshimi K, Haraguchi T, Hanada S. *Mater Trans* 2004;45:365.

[24] Yoshimi K, Hanada S. In: Darolia R, Lewandowski, JJ, Liu CT, Martin PL, Miracle DB, Nathal MV, editors. Proc. 1<sup>st</sup> Int. Symp. Structural Intermetallic Alloys, 1993. p.475.

**Fig. 1**

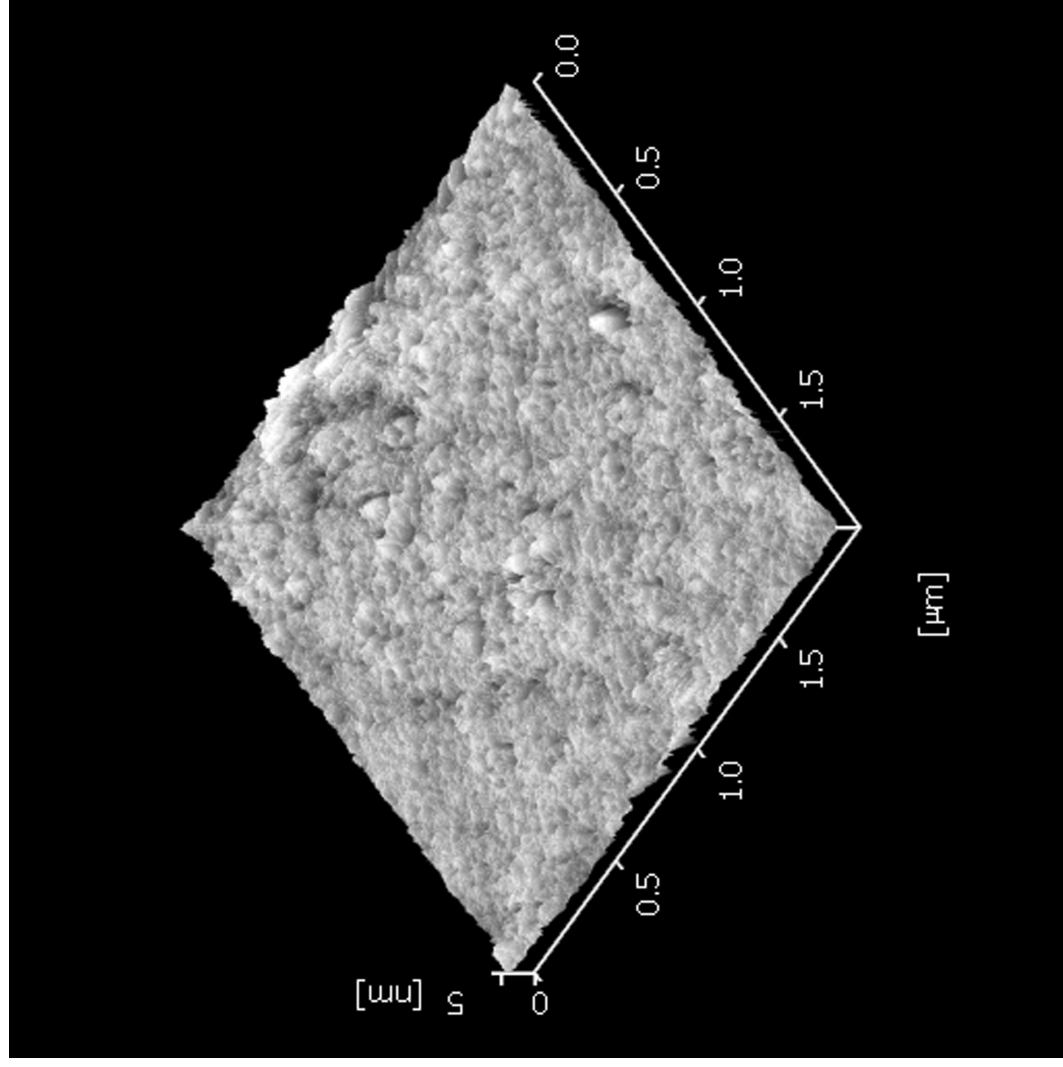


Fig. 2

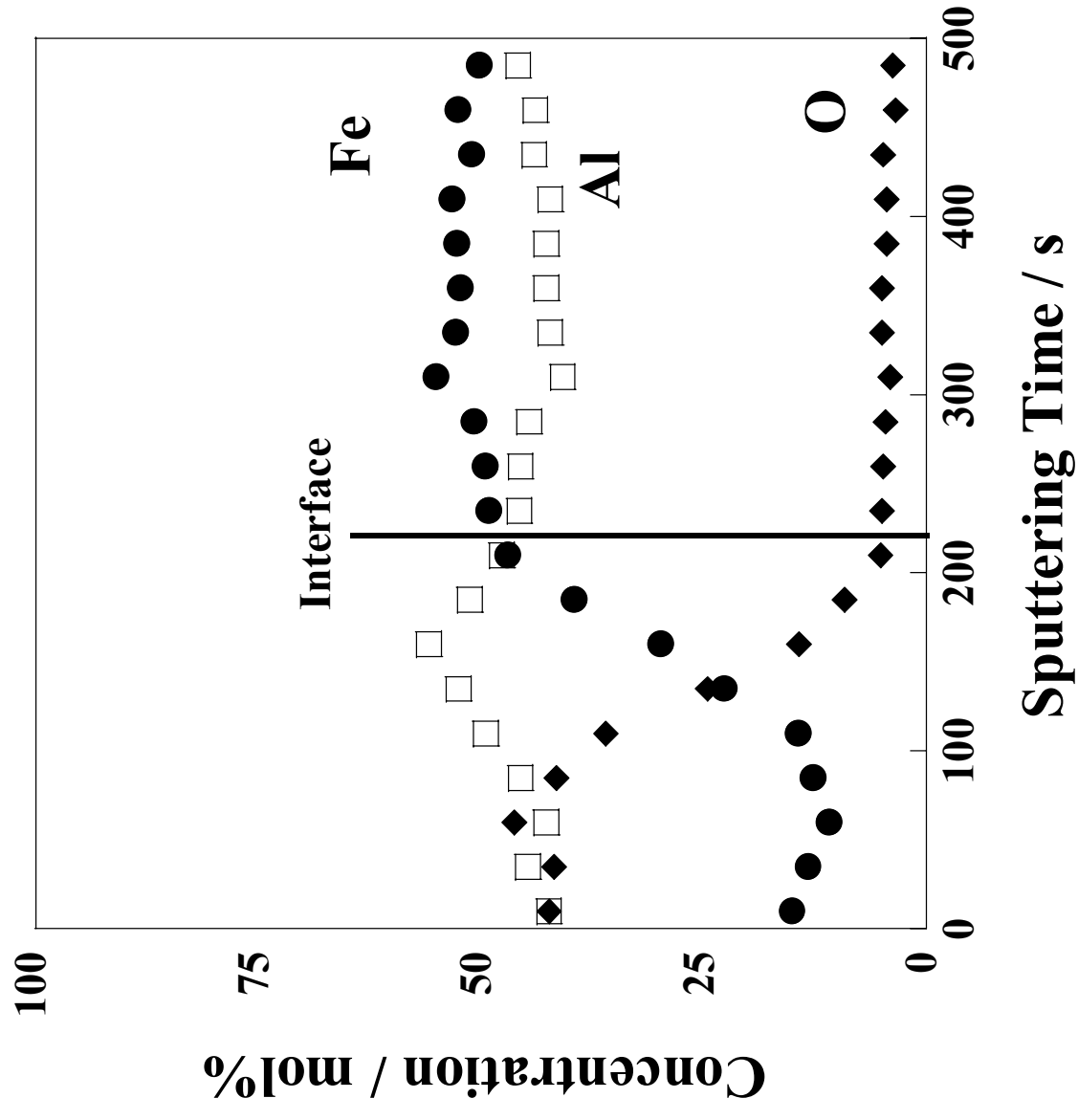
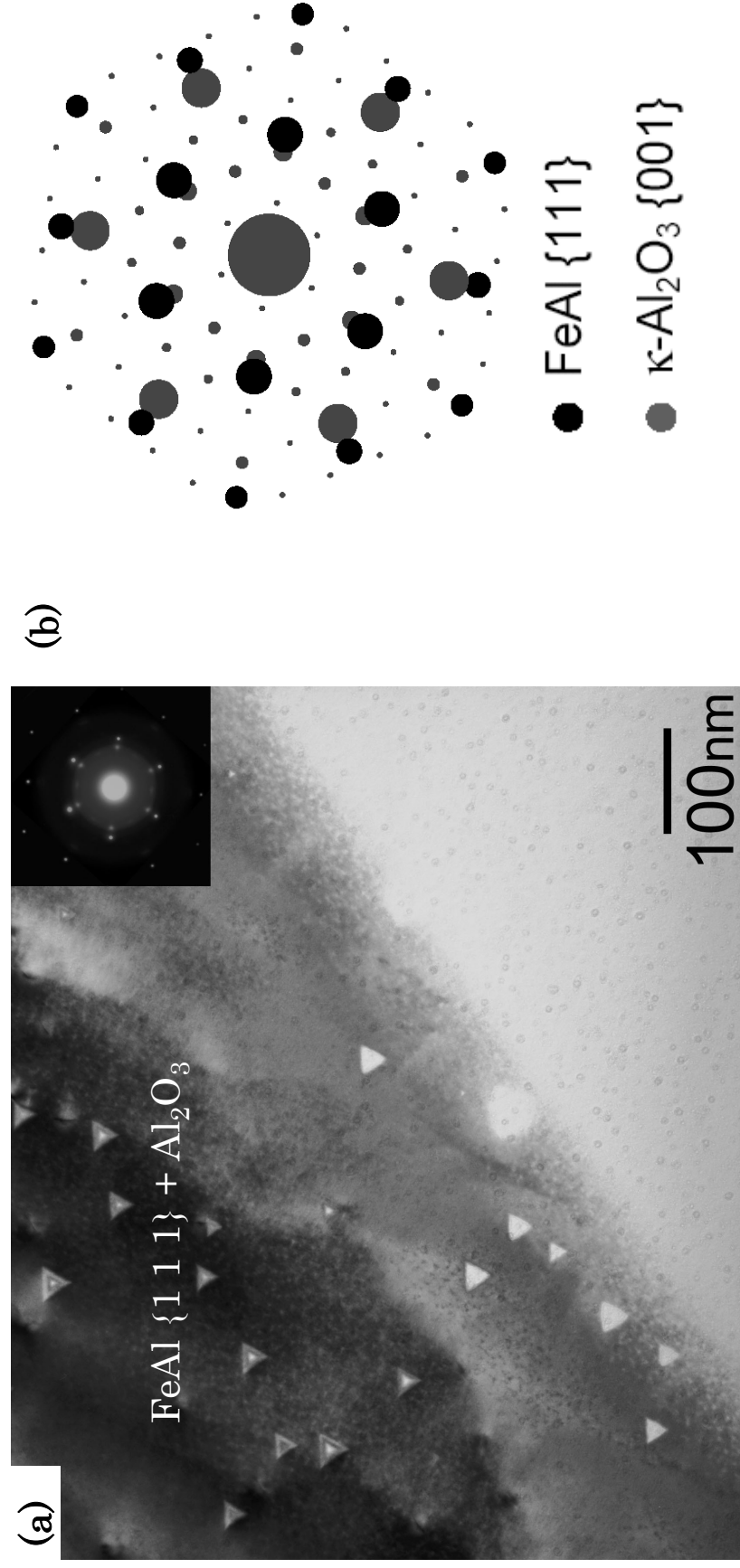
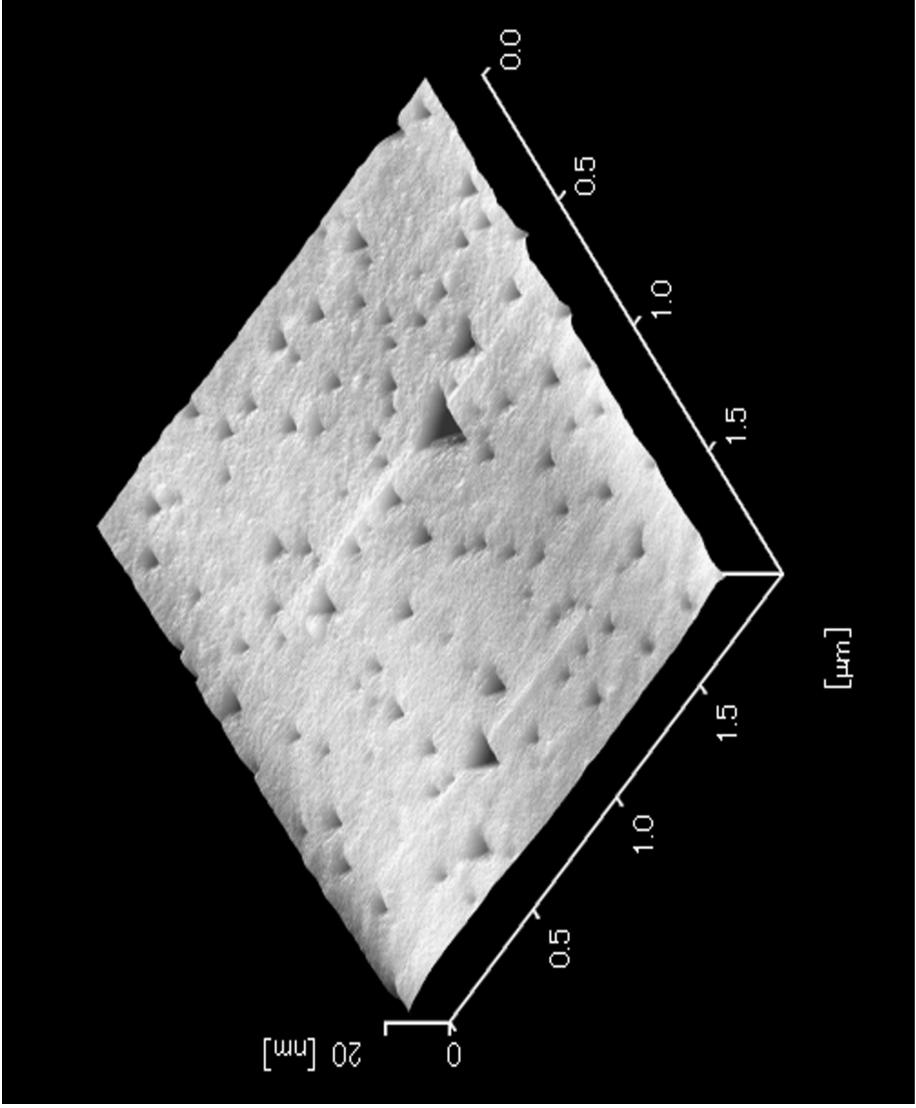


Fig. 3





**Fig. 4**

Fig. 5

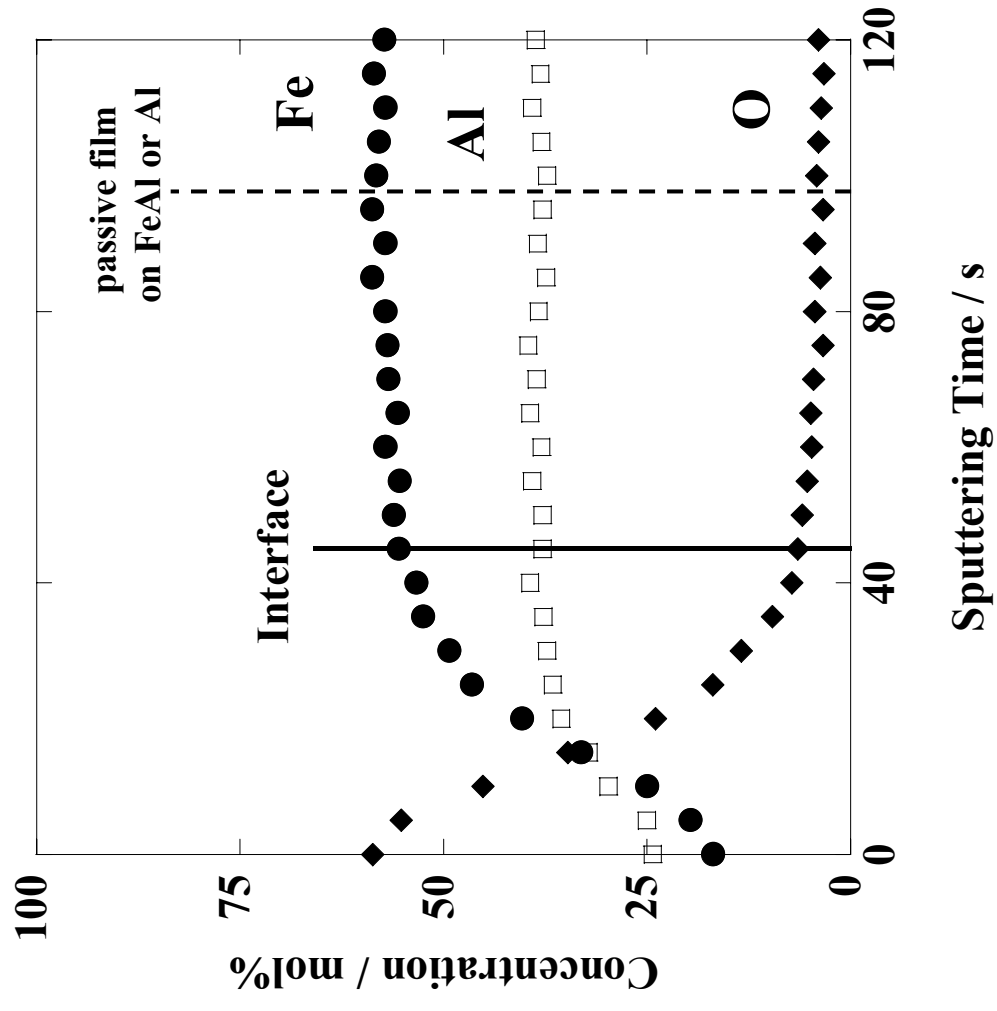


**Fig. 6**

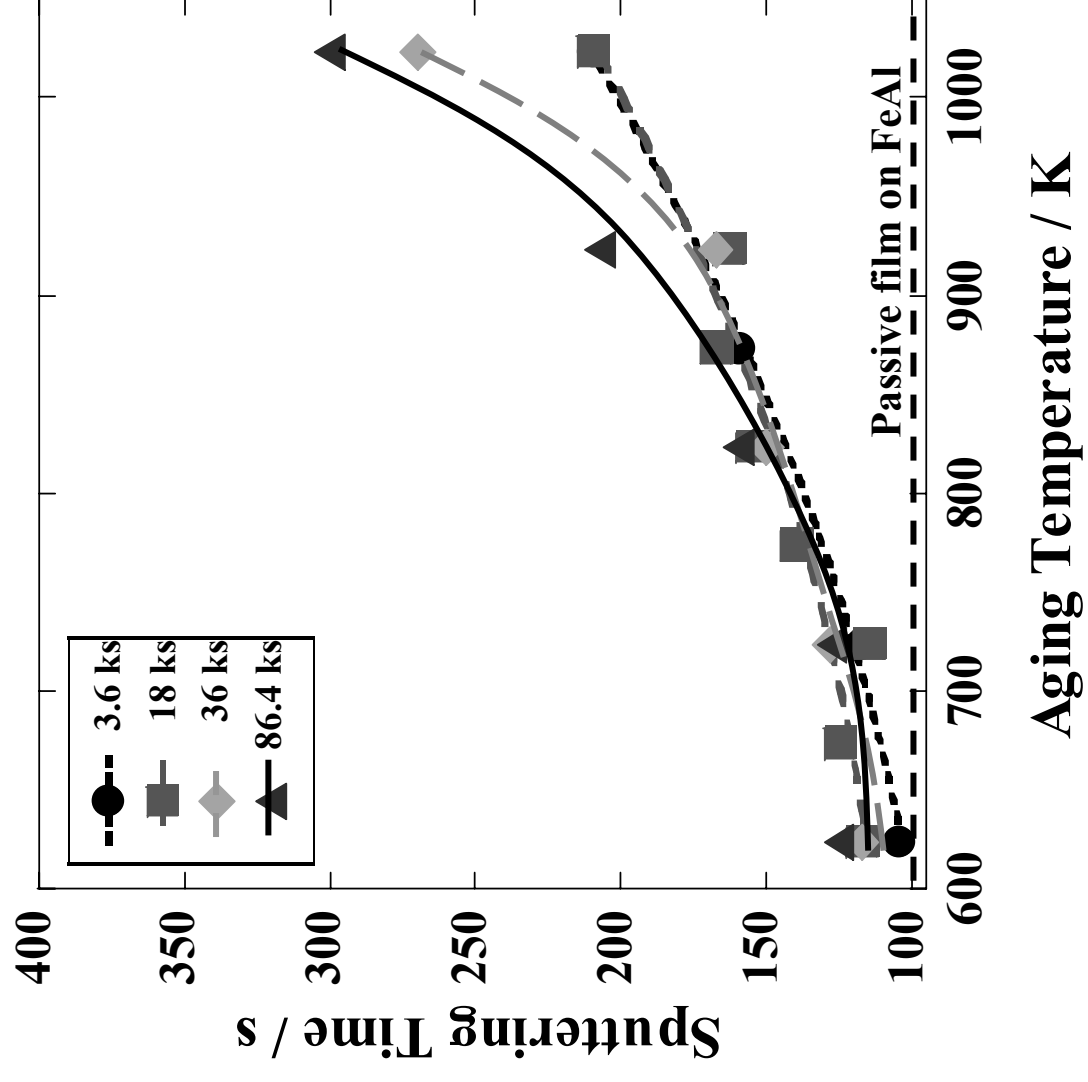
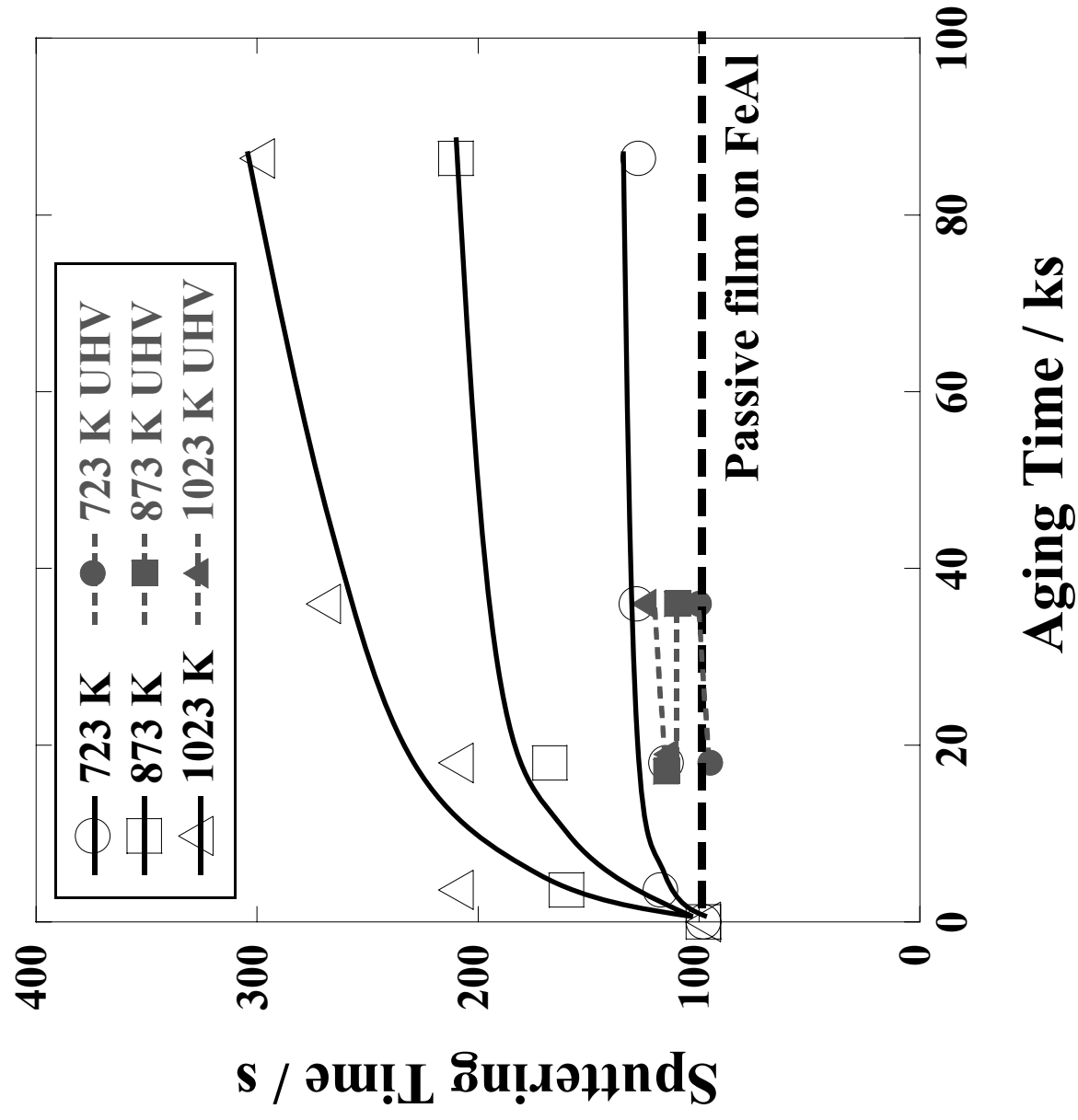


Fig. 7



**Fig. 8**

